BEAM-BASED MEASUREMENTS

I. Agapov, M. Aiba, R. Calaga, B. Dehning, S. Fartoukh, A. Franchi, K. Fuchsberger, M. Giovannozzi, V. Kain, M. Lamont, A. Morita, L. Ponce, S. Redaelli, F. Roncarolo, Y. Sun, R. Tomás, G. Vanbavinckhove, W. Venturini-Delsolaro, J. Wenninger and F. Zimmermann

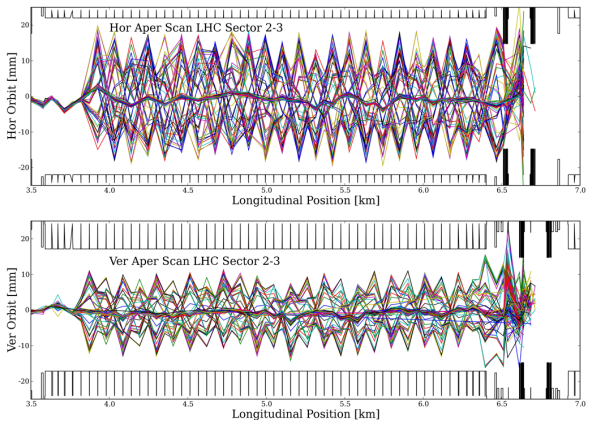

Figure 1: Horizontal (top) and vertical (bottom) orbits recorded during the aperture clearance measurement of the sector 23 Beam 1.

Abstract

A variety of beam-based measurements in the first days of LHC operation was effective to measure aperture clearance, magnet polarities and machine optics. A summary of these measurements is given together with model insights.

INTRODUCTION

During the synchronization tests performed in August-September 2008, aperture clearances, magnet polarities and ring machine optics were measured using beam data. Detailed descriptions of these measurements can be found in [1, 2, 3, 4].

LHC has tight physical apertures by design and therefore the verification of the aperture clearance with beam is a required step to guarantee the machine protection and its performance. Two procedures were used to measure apertures during the synchronization tests:

- Free betatron oscillations generated with two orthogonal orbit correctors to allow a scan in the initial phase. Figure 1 displays all the horizontal and vertical orbits recorded during the sector 23 Beam 1 aperture measurement together with the design apertures. Further information on these measurements can be found in Ref. [1].

- Closed orbit bump with maximum excursion at a suspected aperture bottleneck. Figure 2 displays the beam losses as a function of vertical bump amplitude at the quadrupole MQ.7L3.B1. The design aperture of this quadrupole is 17mm while the measured beam clearance is 12mm. The difference should correspond to the beam size but more precise calculations require accurate knowledge of optics and emittances.

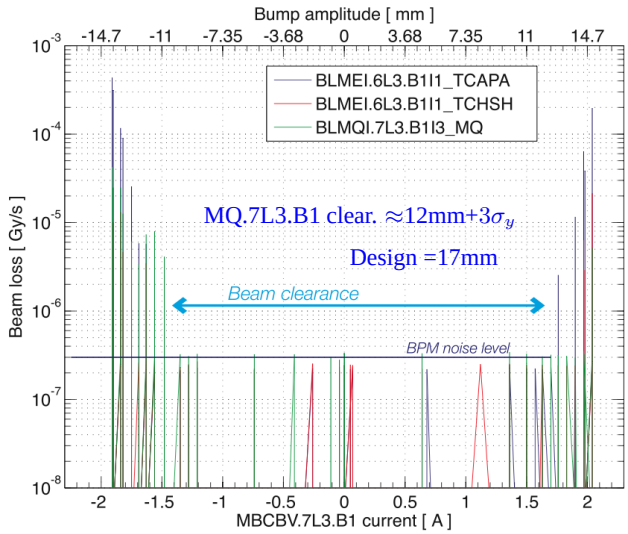

Figure 2: Aperture clearance measurement via a vertical orbit bump scan at MQ.7L3.B1. Design and measured values for the clearance are displayed on the plot. This measurement was performed on the 10^{th} of August 2008.

The importance of verifying magnet polarities is illustrated by the fact that the first inverted polarity found (QTL11.R2B1) [2] together with probe measurements of warm quadrupoles in the collimation insertions and other model considerations led to the discovery of a wrong polarity convention for about half of the trim coils of the LHC [5]. Polarities of several trim quadrupoles, sextupoles and octupoles in the control system were compared to those in the MADX model using beam-based trajectory measurements. Difference trajectories for two settings of each circuit were recorded while launching betatron oscillations via individually selected orbit correctors with optimum phase advance to the magnets of interest. The highlights of these measurements are given in the next section.

The few days devoted to beam commissioning served to establish circulating beam giving the opportunity to verify the periodic ring optics. After many years of study, the procedures to measure and correct the optics of the LHC have been established via numerical simulations and measurements in existing accelerators [6, 7, 8, 9]. The LHC has a beta-beating tolerance lower than any other previous

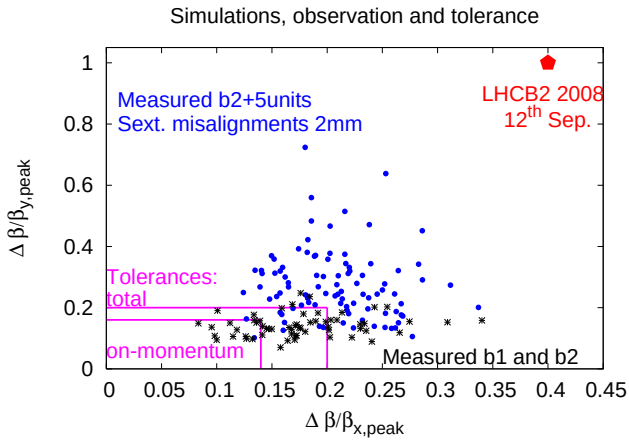

Figure 3: Simulations, observation and tolerances of the peak beta-beating in the LHC, showing an unexpectedly large measured beta-beating in Beam 2.

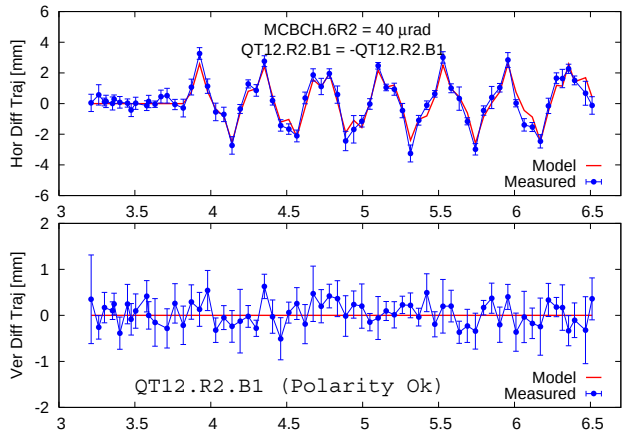

Figure 4: A polarity check showing a good agreement between model and measurement for a trim quadrupole in sector 23 Beam 1.

hadron collider. This requires the use of the most precise numerical algorithms, as well as a highly-performing BPM system. During September the 12$^{\text{th}}$ of 2008, Beam 2 was circulating in the LHC with an excellent lifetime [10]. The turn-by-turn beam position of first 90 turns at about 500 double plane BPMs were acquired using the YASP [11] software. The analysis of these injection oscillations provided the first LHC beta-beating measurement [4]. Figure 3 compares the observed peak beta-beating with previous simulations and the tolerances as presented in Ref. [12]. The Beam 2 LHC optics are not within these initial expectations. This suggests that important optical errors might exist. New algorithms have been used to identify gradient errors from this first measurement of the beta-beating in the LHC.

POLARITY CHECKS

During the injection tests in Sectors 23 and 78 the polarities of several magnets were tested with dedicated beam measurements [2, 3]. To illustrate a positive polarity check, a comparison between measurement and model of the difference trajectory for two settings of QT12.R2B1 is shown in Fig. 4. The horizontal orbit corrector MCBCH.6R2 was used to generate a free betatron oscillation. The polarity and the amplitude of the trajectory is verified to be in agreement with LSA database convention.

Figure 5 illustrates the case where a disagreement in the polarity convention is found. This corresponds to a skew sextupole circuit of Beam 2, namely KSS.A78B2. This measurement was performed with an off-momentum beam to enhance the sensitivity.

Table 1 summarizes the findings of the polarity checks taking into account the current status of the LSA database, e.g., QTL11.R2B1 is listed as “OK” even though it was found to have opposite polarity since it was corrected in the LSA database after the findings.

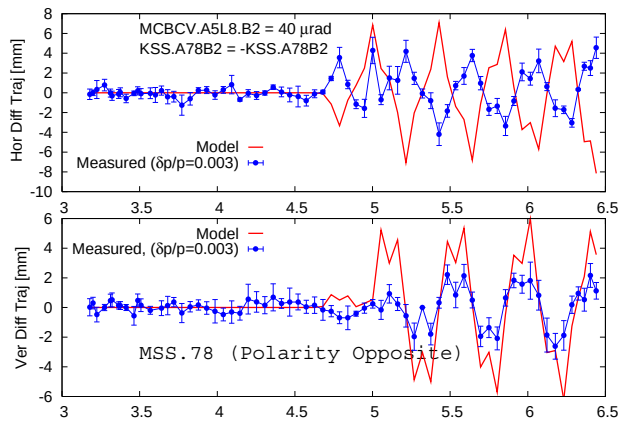

Figure 5: A polarity check showing a disagreement in the polarity convention of a skew sextupole circuit in sector 78 Beam 2.

Polarity disagreement		
MQS23B1	MQS78B2	MSS78B2

Polarity OK		
QTL11.R2B1	QT12R1B1	QT13.R2B1
QT12L8B2	SF[1,2].A23.B1	SF[1,2].A78.B2
SD[1,2].A78.B2	MCS.78B2	KOD.A78B2
KOF.A78B2		

Inconclusive		
QT13.L8B2	KOD.A23B1	

Table 1: Summary of the polarity checks findings taking into account the current status of the LSA database.

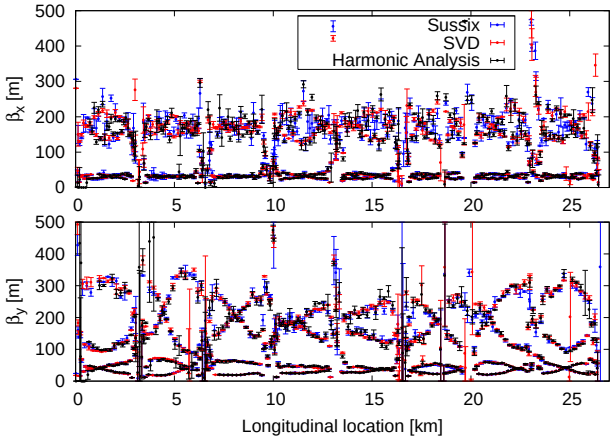

Figure 6: The measurement of the horizontal (top) and vertical (bottom) β functions around the LHC Beam 2.

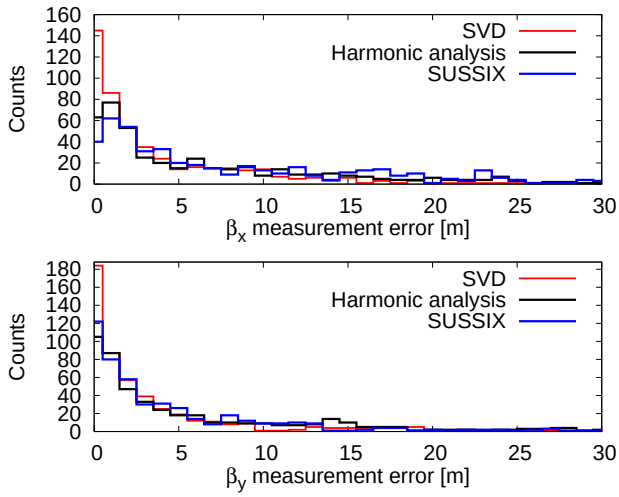

Figure 7: Performance comparison of the three different algorithms used to measure the β functions. Histograms of the horizontal and vertical beta function measurement errors are shown on the top and bottom plots, respectively.

It is important to note that from the set of checked circuits only those of skew magnet type remain with polarity convention disagreements between MAD and LSA. These studies should be pursued and extended to the corresponding magnet circuits in the remaining seven sectors for either beam. Also, the status of the two circuits with so far inconclusive results (see Table 1) needs to be verified.

THE BETA-BEATING MEASUREMENT

The LHC Beam 2 optics measurement was severely constrained due to the availability of a single turn-by-turn BPM data acquisition right at injection and containing only 90 turns. In addition the transverse coupling was uncorrected and the chromaticity was estimated to be 30 units [13]. Despite these set backs, reliable optics measurements were accomplished and described in [4].

The optics is probed through the phase advance between BPMs as this provides a robust and calibration independent observable. The beta functions are extracted from the phase advances between 3 BPMs as it was done in LEP [14]. No statistical error can be assigned to the measurement due to the existence of only a single data acquisition. However by using different combinations of 3 BPMs, different beta functions measurements can be obtained at the same BPM. The average and rms of these measurements yield the beta function and its error bar, respectively.

Three different algorithms are used to measure the phase advance between BPMs, namely SVD [15], SUSSIX [16] and harmonic analysis (or DTFT). The three algorithms yield consistent beta function measurements as shown in Fig. 6. However the SVD approach features a more accurate measurement as displayed in the histograms of the beta functions error, Fig. 7. The better performance of the SVD algorithm can be attributed to the fact that it takes advantage of the correlation between a large set of BPMs as in the case of the LHC. The SVD measurement is used as the reference in the rest of the paper.

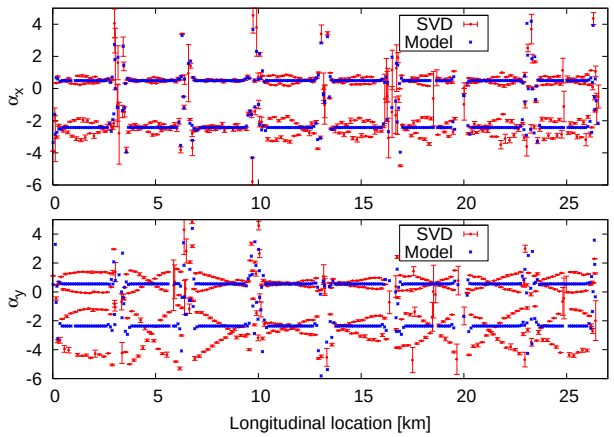

Figure 8: The measurement of the horizontal (top) and vertical (bottom) α functions around the LHC Beam 2 together with the design values.

Alpha functions can be measured in the same way as beta functions, Fig. 8. Although $\alpha_{x,y}$ contain the same qualitative information as the $\beta_{x,y}$, having both measurements turns out specially useful in finding gradient errors as explained in the next section.

The beta-beating is the relative deviation of the measured betas from the design betas. Figure 9 compares the LHC Beam 2 observed beta-beating to the tolerances. The horizontal beta-beating is within expected values for a first measurement and not far from tolerances. However the large vertical beta-beating cannot be explained neither by the measured multipolar components of the superconducting magnets, nor by the observed closed orbit distortion, see Fig. 10. New algorithms have been developed in order

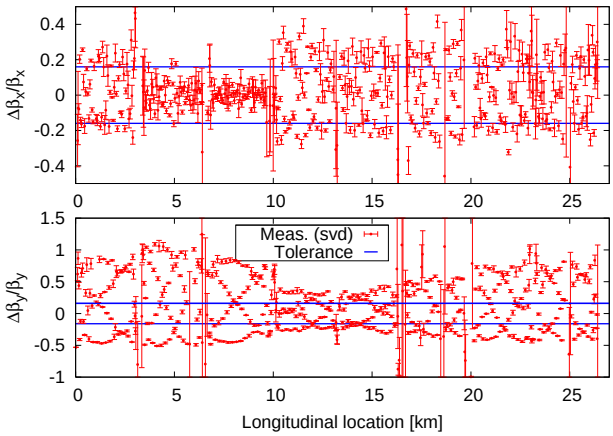

Figure 9: Measured horizontal (top) and vertical (bottom) beta-beating versus longitudinal location together with tolerances.

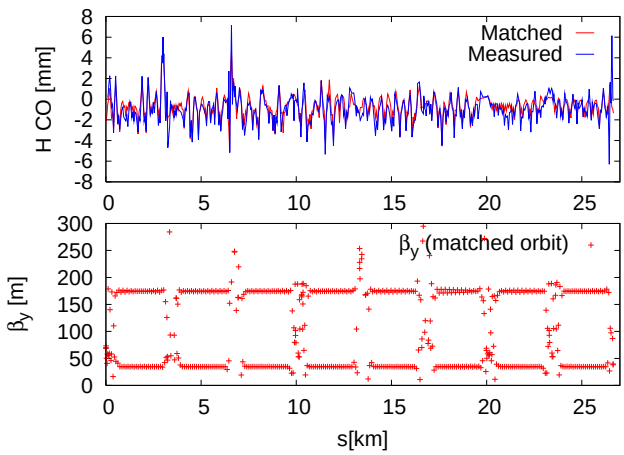

Figure 10: Top: measured and matched horizontal closed orbit. Bottom: The vertical beta function for the model including the matched orbit, having a negligible beta-beating.

to identify possible gradient errors.

OPTICS ERRORS RECONSTRUCTION

A typical approach for optics correction in accelerators uses the inverse model response matrix of gradient strengths on some observables like phase advances, beta functions or dispersion, see e.g. [7, 17, 18]. This is illustrated by the following equation,

$$\begin{pmatrix} \Delta\phi_1 \\ \Delta\phi_2 \\ \Delta\phi_3 \\ \vdots \\ \Delta\phi_N \end{pmatrix} = \mathbf{R} \times \begin{pmatrix} \Delta K_1 \\ \Delta K_2 \\ \Delta K_3 \\ \vdots \\ \Delta K_M \end{pmatrix}, \qquad (1)$$

where $\mathbf{R}$ is a rectangular matrix,

$$\mathbf{R} = \begin{pmatrix} R_{11} & R_{12} & R_{13} & \cdots & R_{1M} \\ R_{21} & R_{22} & R_{23} & \cdots & R_{2M} \\ R_{31} & R_{32} & R_{33} & \cdots & R_{3M} \\ \vdots & \vdots & \vdots & \ddots & \vdots \\ R_{N1} & R_{N2} & R_{N3} & \cdots & R_{NM} \end{pmatrix},$$

ϕ_i represent the N phase advances between BPMs, K_i correspond to the M gradient variables and $\mathbf{R}$ is the model response matrix that connects them. This approach is not suitable for this exceptional situation where the size of the errors exceeds the linear regime and there is no possibility to iterate corrections on the machine.

A more local approach aiming at identifying errors has been developed. The entire machine is split into several segments and each of these segments is treated as an independent transfer line. The measured alpha and beta functions at the entrance of the segment are used as initial conditions for the optics of the respective segment. The propagation of the initial conditions using the ideal model should follow the measurement as far as there are no gradient errors. Therefore, any deviation from the measured optics is easily identified by a direct comparison, thus localizing the gradient error. The strength of the errors within the segment can be determined by matching the propagated optics to the measured optics via the preferred matching algorithm. The advantage of having a segmented machine is the considerable reduction of the dimensionality of the problem. Therefore, only the matching variables within the segment are used to reconstruct the measured optics. Following the illustration of Eq. (1), by having changed the reference model in every segment we have transformed the $\mathbf{R}$ matrix into a block diagonal matrix, with n independent blocks, represented by the independent response matrices $\mathbf{R_i}$,

$$\mathbf{R} = \begin{pmatrix} \mathbf{R_1} & \mathbf{0} & \mathbf{0} & \cdots & \mathbf{0} \\ \mathbf{0} & \mathbf{R_2} & \mathbf{0} & \cdots & \mathbf{0} \\ \mathbf{0} & \mathbf{0} & \mathbf{R_3} & \cdots & \mathbf{0} \\ \vdots & \vdots & \vdots & \ddots & \vdots \\ \mathbf{0} & \mathbf{0} & \mathbf{0} & \cdots & \mathbf{R_n} \end{pmatrix}.$$

This method naturally applies to LHC by splitting the ring into IRs and arcs. It is important to verify that the measured betas and alphas used as initial conditions for the propagated optics have low measurement errors. This can be easily checked by changing the initial conditions according to the errors and compare the propagated optics.

This method proved most useful for the IR3. This segment consists of about 20 quadrupoles as shown on the top plot of Fig. 11. The two bottom plots show the horizontal and vertical beta functions from measurement and for two models (propagated by taking the initial α and β as measured). The ideal model is represented by the blue stars which shows an excellent agreement with the measurement until the location 10200 m, where the vertical beta func-

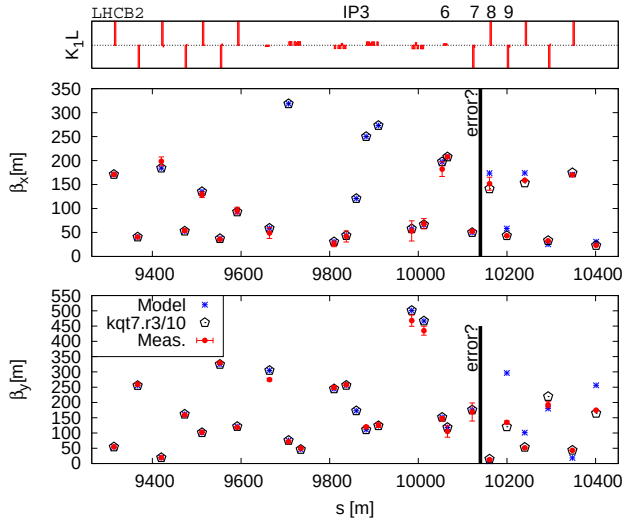

Figure 11: Segment-by-segment approach in IR3. The top plot shows the gradient distribution versus longitudinal location. The two bottom plots show the horizontal and vertical beta functions from measurement and for two models (propagated by taking the initial α and β as measured). The model with a tenth of the strength of mqtli7 shows a much better agreement.

tions largely differ. This suggests that a gradient error exists between the 6^{th} and the 9^{th} quadrupoles (as indexed on the top plot). To restore the good agreement between model and measurement the quadrupole mqtli7r3b2 had to be switched off or reduced by a factor of ten (black pentagons on the figure), clearly suggesting some hardware problem with this quadrupole. This same feature was also observed from dispersion measurements in Ref. [19]. The most likely hypothesis to explain this observation was the cable swap between the magnets of the two beams, namely mqtli7r3b2 and mqtli7r3b1. This hypothesis was confirmed from previous hardware tests, which revealed a voltage inversion between the corresponding voltmeters [20]. However the results from these new analyzes were crucial to determine that the voltmeters were actually properly connected and that there was a real cable swapping problem between magnets.

The segment-by-segment method is also applied to other sectors. Table 2 summarizes the current status of the findings. It is clear that the error found in IR3 is the most important producing by itself more than 50% peak beta-beating in the vertical plane. The rest of the errors can only be considered as a "best fit" and need further investigation.

Figure 12 compares the model after including all the findings from the segment-by-segment approach to the measurement. The agreement is not fully satisfactory in the vertical plane most likely due to existance of other, probably, smaller errors.

Yet a new method has been implemented to achieve the best possible optics error reconstruction. This method is based in the already mentioned inverse model response matrix (using the closed solution), Eq. (1), but with an important new feature to allow for iterations. After each iteration the change in the model phase advance (obtained by introducing the corrections in the ideal model) is subtracted to the measured phase advances as a means to simulate an iterative correction in the real machine.

Segment	$\frac{\Delta\beta_x}{\beta_x}$ peak [%]	$\frac{\Delta\beta_y}{\beta_y}$ peak [%]	Source (change)
IR3	17	54	mqtli7r3b2 (/10)
IR2	9	5	mqya4l2b2 (+14%)
IR7	6	6	mqt5[rl]7 ($\times$[-2,3])
IR6	5	4	mq4l6b2 (+1%)
ARC23	0	3	mqd23 (+0.4%)

Table 2: Segment-by-segment summary. The second and third columns show the impact of the error by itself in the ideal lattice. The first and fourth columns show the segment and the "best fit" corrector. Only the IR3 error has been confirmed as a real error.

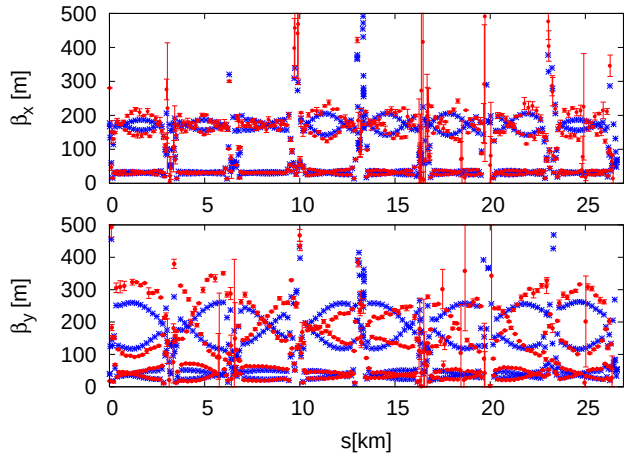

Figure 12: Comparison of measured beta functions and the model after including all the findings from the segment-by-segment.

To obtain the best possible results we have applied this new model iterative correction starting from a model already including the segment-by-segment findings. After five iterations a very satisfactory agreement is found between model and measurement, Fig. 13. The qualitative summary of the integrated strengths used in the correction is shown in Fig. 14.

It is reassuring to observe that the IR3 error remains as the strongest one and that no other relevant error has been found in IR3 by the iterative approach. However IR2 seems to need further investigations since the iterative correction finds comparable errors to those suggested by the segment-by-segment. It is also patent that IR1, IR5 and IR8 have very low optics errors.

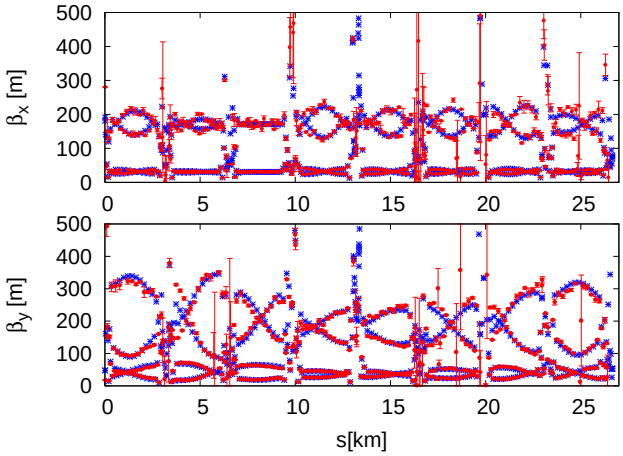

Figure 13: Comparison of model and measured beta functions after five iterations of the model iterative correction (having started from the segment-by-segment results).

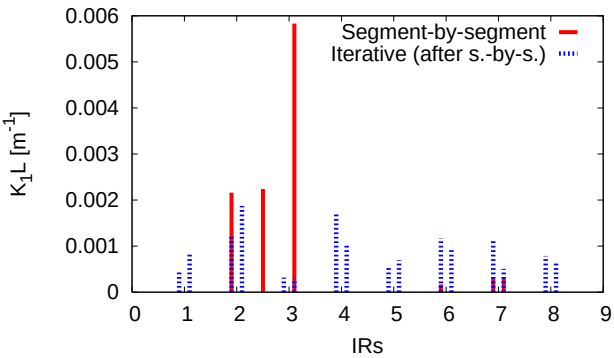

Figure 14: Integrated error distribution as obtained by the segment-by-segment and the iterative approaches.

COUPLING

The linear coupling parameters are inferred from the secondary spectral lines, i.e. the vertical tune in the horizontal signal and vice-versa, see e.g., Ref. [21]. Figure 15 compares the real part of the difference coupling resonance driving term f_{1001} with a fitted model. The five periods observed in the oscillations of the real part of f_{1001} correspond exactly to the integer tune split between the horizontal and vertical tunes, thus experimentally confirming that the machine had the same integer tune split as the model.

Linear coupling is generated by the rotation of quadrupole magnets, a nonzero vertical closed orbit at the sextupoles and the a_2 magnetic errors in the superconducting dipoles. There were no skew quadrupole correctors excited during the measurement. Repeating this measurement with better quality data should give an insight into the sources of coupling guided by theory [21] and simulations [7].

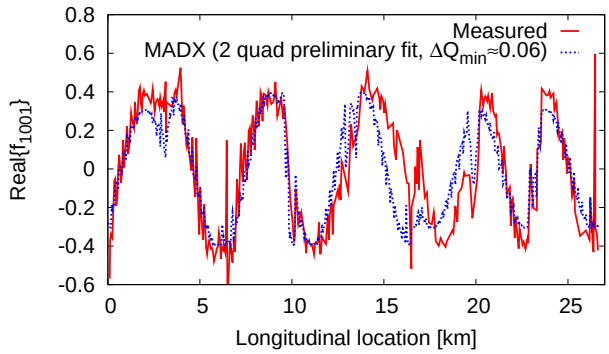

Figure 15: Real part of the coupling resonance driving term f_{1001} compared with a model prediction that is obtained by exciting two skew quadrupoles to approximately reproduce the measurement.

SUMMARY

Beam-based measurements are vital to reach the nominal performance and safety of the LHC rapidly. During the synchronization tests well established aperture measurement techniques were tested and successfully applied to two sectors of the machine.

Polarity checks with beam were crucial in finding important polarity convention disagreements and to verify the good functioning of many fundamental circuits. It was demonstrated that the polarity and the strength (at the level of 10%) of higher order corrector circuits - sextpoles, b_3 spool pieces, skew sextupoles, Landau octupoles - can easily be measured at injection energy for each individual sector. The fact that the circuits of skew magnet type were found to have a convention disagreement calls for the establishment of a proper model description that takes into account the magnet orientation and the powering criteria. These beam-based measurements should continue until the full certitude on aperture clearance and polarities is accomplished.

The only turn-by-turn BPM data acquisition at injection has served to test and compare various methods to measure the periodic ring optics. In the constrained circumstances with only 90 turns, uncorrected coupling and large chromaticity, the SVD approach proved to be the most accurate. The measured vertical beta-beating is found to be larger than predicted by the specified field and alignment errors, suggesting that a few additional large error sources may exist. Two new methods to address the localization of optics correction were developed, namely segment-by-segment and model iterative correction. The application of the segment-by-segment approach to IR3 led to the identification of a dominant optics error in LHC Beam 2. Evidence from previous hardware tests supported the hypothesis that this error was caused by a cable swapping between the Beam 2 and Beam 1 magnets MQTLI7R3B2 and MQTLI7R3B1. The model iterative correction has confirmed that there are no more relevant errors in IR3, IR1,

IR5 and IR8. However it is important to note that due to the Beam 1 - Beam 2 powering symmetry in IR1 and IR5, cable swapping problems may exist. Dedicated measurements should be pursued in the future to clarify the appropriate cabling. The error sources in IR2 still remain unclear and further investigations are needed.

ACKNOWLEDGMENTS

These data only exist due to the exceptional work of the LHC operation and instrumentation teams. We thank O. Brüning for the supervision of this work. We are thankful to E. Calvo Giraldo and R. Jones for providing feedback on the BPM status. Thanks to N. Catalán Lasheras for providing the critical information concerning the results of the hardware tests of mqtli7r3b2. Thanks to Y. Papaphilippou, S. Peggs, F. Schmidt and R. Steinhagen for the very useful discussions.

REFERENCES

[1] O. Aberle *et al.*, "The LHC Injection Tests", LHC-Performance-Note-001, (2008).
http://cdsweb.cern.ch/record/1125992/files/performance-note-001.pdf

[2] K. Fuchsberger, V. Kain, M. Lamont, L. Ponce, W. Venturini-Delsolaro, J. Wenninger, A. Butterworth, S. Fartoukh, R. Tomás and F. Zimmermann, "Trim Magnet Polarities, Dispersion, and Response Data in Sector 23", LHC-Performance-Note-002, (2008).
http://cdsweb.cern.ch/record/1132354/files/performance-note-002.pdf

[3] R. Calaga, V. Kain, M. Lamont, L. Ponce, Y. Sun, R. Tomás, W. Venturini-Delsolaro, F. Zimmermann, "Polarity checks in sectors 23 & 78", LHC-Performance-Note-010, (2009).
http://cdsweb.cern.ch/record/1163686

[4] M. Aiba, R. Calaga, A. Franchi, M. Giovannozzi, V. Kain, A. Morita, R. Tomás, G. Vanbavinckhove and J. Wenninger, "First Beta-Beating Measurement in the LHC", LHC-Performance-Note-008, (2009).
http://cdsweb.cern.ch/record/1157249/files/performance-note-008.pdf

[5] Hypothesis elaborated by S. Fartoukh, minutes of the LHC Performance Committee 2008-02, 20$^{\text{th}}$ of August 2008:
https://ab-div.web.cern.ch/ab-div/Meetings/lhcperc/

[6] F. Zimmermann, S. Fartoukh and R.W. Assman, "Measuring beta functions and dispersion in the early LHC" EPAC 2002.
http://accelconf.web.cern.ch/AccelConf/e02/papers/mople031.pdf

[7] R. Tomás, O. Bruning, R. Calaga, S. Fartoukh, A. Franchi, M. Giovannozzi, Y. Papaphilippou, S. Peggs and F. Zimmermann, "Procedures and accuracy estimates for beta-beat correction in the LHC" EPAC 2006.
http://accelconf.web.cern.ch/AccelConf/e06/papers/wepch047.pdf

[8] R. Calaga, R. Tomás and F. Zimmermann, "BPM calibration independent LHC optics correction", PAC 2007.
http://accelconf.web.cern.ch/AccelConf/p07/papers/thpas091.pdf

[9] M. Aiba, R. Calaga, A. Morita, R. Tomás and G. Vanbavinckhove, "Optics correction in the LHC", EPAC 2008.
http://accelconf.web.cern.ch/AccelConf/e08/papers/wepp025.pdf

[10] L. Evans, "LHC commissioning & status", presented in the 9$^{\text{th}}$ ICFA seminar:
http://www-conf.slac.stanford.edu/icfa2008/agenda.asp

[11] J. Wenninger, "YASP: Yet Another Steering Program"

[12] S. Fartoukh and O. Brüning, "Field Quality Specification for the LHC Main Dipole Magnets" CERN-LHC Project Report-501 (2001).
http://cdsweb.cern.ch/record/522049/files/lhc-project-report-501.pdf

[13] A. Boccardi, M. Gasior, O. R. Jones, P. Karlsson and R. J. Steinhagen, "First Results from the LHC BBQ Tune and Chromaticity Systems", LHC-Performance-Note-007, (2009).
http://cdsweb.cern.ch/record/1156349/files/performance-note-007.pdf

[14] P. Castro-Garcia, "Luminosity and beta function measurement at the e-e+ collider ring LEP" Ph.D. Thesis, CERN-SL-96-70-BI (1996).
http://ccdb4fs.kek.jp/cgi-bin/img_index?9701158

[15] R. Calaga, "Linear Beam Dynamics and Ampere Class Superconducting RF Cavities at RHIC", Ph.D. Thesis, Stony Brook university, 2006.
http://www.agsrhichome.bnl.gov/People/rcalaga/thesis.html

[16] R. Bartolini and F. Schmidt, "A Computer Code for Frequency Analysis of Non-Linear Betatron Motion" SL-Note-98-017-AP.
http://sl.web.cern.ch/SL/Publications/ap98-017.pdf

[17] A. Morita, H. Koiso, Y. Ohnishi and K. Oide, "Measurement and correction of on- and off-momentum beta functions at KEKB", Phys. Rev. ST Accel. Beams **10**, 072801 (2007).

[18] D. Sagan, R. Meller, R. Littauer, and D. Rubin, "Betatron phase and coupling measurements at the Cornell Electron/Positron Storage Ring", Phys. Rev. ST Accel. Beams **3**, 092801 (2000).

[19] M. Lamont, "LHC dispersion measurements 2008 revisited", LHC-Performance-Note-009, (2009).
http://cdsweb.cern.ch/record/1157956/files/performance-note-009.pdf

[20] N. Catalán Lasheras, private communication, January 2009.

[21] R. Calaga, R. Tomás and A. Franchi, "Betatron coupling: Merging Hamiltonian and matrix approaches" Phys. Rev. ST Accel. Beams **8**, 034001 (2005).